

# Elemental analysis of Kimberlite and associated Country Rock

Marius Tchonang<sup>1</sup>, Martin Cook<sup>1</sup>, Faan Bornman<sup>2</sup>, Simon Connell<sup>1</sup>  
and Sergio Ballestrero<sup>1</sup>

<sup>1</sup> Physics Department, University of Johannesburg, PO Box 524 Auckland Park

<sup>2</sup> Multotec Process Equipment (Pty) Ltd

E-mail: mariust82@gmail.com

**Abstract.** The elemental analysis of kimberlite and country rock was performed as part of an ongoing study into the Mineral-PET online rock sorting technique. This is a technology proposed to locate high densities of carbon in kimberlite and country rock using the very well known medical physics technique called Positron Emission Tomography (PET). Carbon in kimberlite is not a natural positron emitter; one has to convert the naturally occurring carbon into a positron-emitting isotope. In this case it is done through the photo-nuclear transmutation reaction  $^{12}\text{C}(\gamma, n)^{11}\text{C}$ . We accomplish this reaction by irradiating the host rock using gamma rays with energies in the Giant Dipole Resonance (GDR) region. It is then important to determine the full inventory of radioisotopes produced in this process. The irradiation of kimberlite was performed using the 100 MeV electron microtron at Aarhus University in Denmark. In this paper, we first describe the experiment, and then perform an analysis of the data. This provides quantitative identification of the prompt, short, mid-term and even long-term radioactivity of irradiated kimberlite. This is necessary in order to assess more efficiently the radiation safety of the equipment and people working in the facility. A unique feature of this analysis is the unambiguous identification and quantification of each radioisotope formed by the two dimensional spectroscopy of the energy and the emission time of the signature gamma lines using time differential spectroscopy.

## 1. Introduction

The extraction of diamonds from excavated rocks has to date been an uneconomical process requiring lot of energy. In a typical diamond mine, the rocks are first coarse-crushed into pieces of about 10 to 15 cm diameter and then ultimately crushed into pieces of some few millimetres. It is then assumed that most of the diamonds will be liberated or exposed at the surface. Different techniques are then used to extract them [1]. This method is inefficient since only a small fraction of the rock contains diamond. Mineral-PET proposes a more economical method where, after the coarse crush, only diamond bearing rock could be further processed. A similar approach has been used in the well known medical Positron Emission Tomography (PET), but rather than introducing the positron emitter in the patient, it is produced within the host rock by irradiating it with a photon beam with energies in the Giant Dipole Resonance (GDR) region [2, 3]. It is important to determine the full inventory of radioisotopes produced in the irradiation process. The irradiation was performed using the 100 MeV electron microtron at Aarhus University in Denmark. Time differential gamma-ray spectroscopy is used to identify the peaks of the spectrum. The possible primary reactions in the host rock are  $(\gamma, n)$ ,  $(\gamma, p)$ ,

$(\gamma, \alpha)$ ,  $(\gamma, 2n)$  and  $(\gamma, n + p)$ . The products of these reactions can interact with the host rock in many other secondary reactions. Furthermore, we assess all the nuclides involved in the activation of kimberlite as the viability of the mineral-PET technique relies on this assessment. The time differential gamma-ray spectroscopy offers the advantage of allowing the identification of active isotopes based on both lifetime and energy, rather than only the energy, which is the only information available in normal gamma ray spectroscopy.

## 2. Experiment

The Aarhus 100 MeV electron Microtron irradiation system is used to irradiate a piece of kimberlite rock. This facility is equipped with an irradiation stage for the samples. The beam energy can be modified by the use of degraders. The electron current and irradiation time are measured. The electron and photon irradiation spectrum distribution is modelled with Monte Carlo transport calculations. The irradiation dose details can therefore be controlled, measured and modelled. In the example below the irradiation condition was 100 MeV electrons incident on a 2 mm stainless steel exit port.

A piece of Kimberlite rock is irradiated, keeping the sample in position in front of the beam exit point. The irradiation time was 1000 s for a dose of  $5.25 \times 10^{13}$  electrons/cm<sup>2</sup>. Note that this is about 17 times the anticipated dose in the Mineral-PET facility[5]. After irradiation, a gamma spectroscopy system based on event-by-event acquisition implemented on a VME standard records time-stamped energy data for each event. The data is analyzed offline in a time differential manner, to provide both the gamma-line energy and lifetime. One detection run therefore yields complete information about both the energies and lifetimes of all isotopes present, allowing for unique isotope identification in most cases.

## 3. Data analysis and results

### 3.1. Method

The time-stamped energy data is collected for each event and a calibrated energy histogram is plotted. From figure 1, the different peaks corresponding to diverse energy lines present in the spectrum can easily be distinguished. The graph in figure 1 presents many peaks with the most visible ones being at 511 keV, 846 keV, 1271 keV, 1365 keV, 1432 keV, 1460 keV, 1730 keV, 2164 keV, 2241 keV and 2754 keV. A time differential energy spectrum of the irradiated kimberlite shows that the height of the peaks varies with time. Figure 2 shows the dominance of the 511 keV peak, and also some very short-lived peaks vanishing before 1000 s. One can also distinguish very long-lived peaks with the intensity remaining almost constant for a few hours. The data is time sliced with different time bin sizes depending on the number of events required to have a histogram representing the different peaks. The peaks are fitted with an asymmetric gaussian and the area under the fit for every time slice is calculated[4]. This yields the peak intensity (area) as a function of the time. The lifetime of each energy line as a function of the time can be extracted from the peak intensity for different time slices. These new data is fitted with an exponential decay. In the cases with interfering peaks, two components in the decay of the line were included. The energy of the line and the half-life yields an unambiguous isotope identification using a database of nuclide level schemes[6].

Figure 3 presents the histograms and the asymmetric gaussian fit for the 511 keV peak for different time slices. The histograms and the fits are stacked, remaining exactly at the position 511 keV. In figure 5, the peak tends to be moving which suggest the 845.8 keV might be a combination of two very close lines with the centres at 844 keV and 846 keV.

### 3.2. Results and discussion

The single decay fit of the 845.8 keV line shown in figure 5 gives a lifetime of 94 minutes with some discrepancies in the early and the latter part of the spectrum. This suggests a two

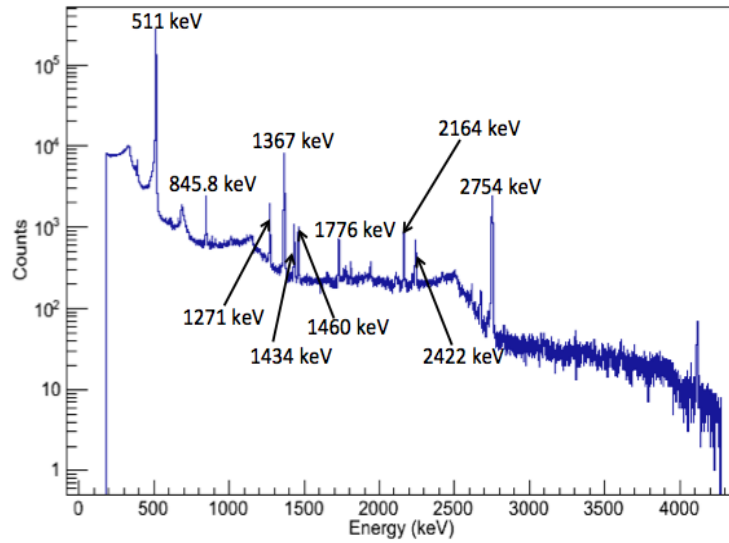


**Figure 1.** Calibrated energy spectrum with the dominance of the 511 keV PET line

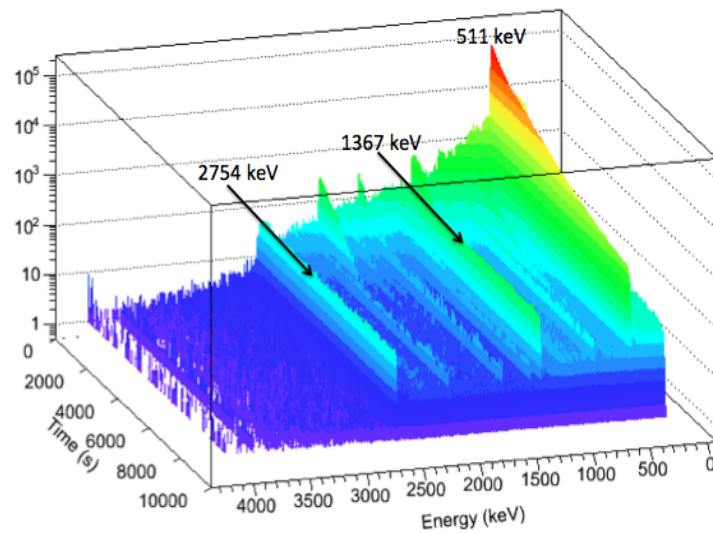


**Figure 2.** Time differential gamma spectroscopy for life-time determination for each gamma-line

component fit of the data. For the long-lived component of the fit, the possible candidates are  $^{87}\text{Kr}$  with lifetime of 76.3 min 9 s and  $^{56}\text{Mn}$  with a lifetime of 2.58 h.  $^{87}\text{Kr}$  could come from neutron absorption on the natural  $^{86}\text{Kr}$  but from the kimberlite composition, it is highly unlikely that krypton could be present in the environment[7].  $^{56}\text{Mn}$  is either from neutron capture on  $^{55}\text{Mn}$  (abundance 100%) which is present in kimberlite or from  $(\gamma, p)$  and  $(\gamma, n + p)$  reactions on different iron isotopes, also present in kimberlite. For the short-lived component, we fixed the long-lived one to  $^{56}\text{Mn}$  and extracted a lifetime of 10 min for the unknown short-lived isotope. Figure 6 shows the two best candidates with lifetimes shorter and longer than 94 minutes, namely  $^{56}\text{Mn}$  with half-life 155 m and  $^{27}\text{Mg}$  with half-life 9.5 m.  $^{27}\text{Mg}$  is probably from neutron capture

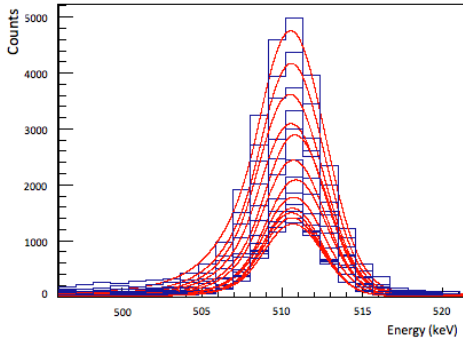


**Figure 3.** Single spectrum for the 511 keV gamma-line for consecutive time slices.

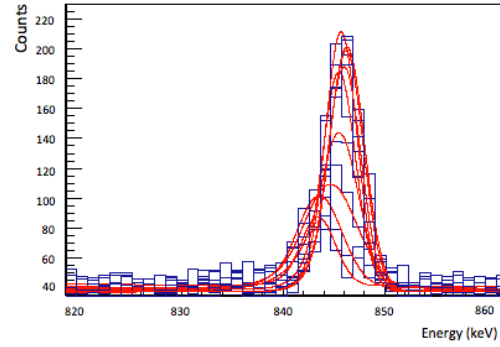


**Figure 4.** Single spectrum for the 845.8 keV gamma-line for consecutive time slices.

on stable  $^{26}\text{Mg}$  or (n,p) reaction on  $^{27}\text{Al}$ .

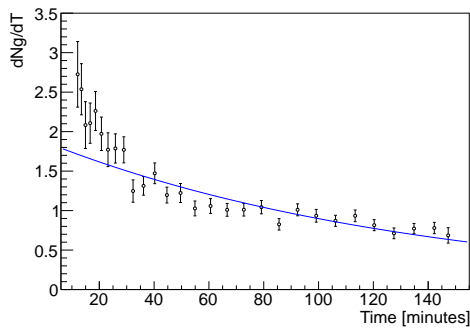


**Figure 5.** One decay best fit of the 845.8 keV signal with the fit missing the data after 100 min.

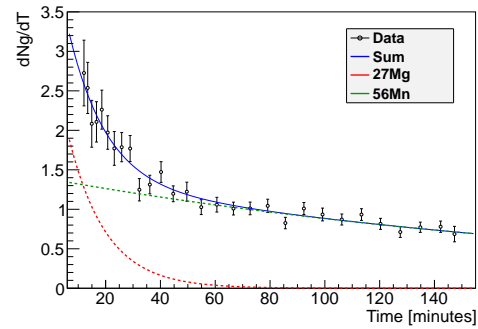


**Figure 6.** Lifetime spectrum of the 845.8 keV signal which is a sum of 2 decays: magnesium and manganese.

Similar procedure allows for the identification other lines and the results are presented in Table 1. There are many other small peaks which are most probably noise from adjacent intense ones. Some of these lines come from the same isotope but at different energy or even from a process known in gamma-ray spectroscopy as single or double escape peaks[8]. This is the case for the 1653 keV and 1143 keV respectively. We also have a peak at 2675 keV which comes from a single pile-up ( 2164 keV collected simultaneously with a 511 keV gamma ray).

**Table 1.** List of peaks with the parents, half-lives and possible processes leading to the isotopes or peaks.

Energy (keV)	Parents	Half-life	Process
511	$^{11}\text{C}$	20min23s	$(\gamma, n)$ on $^{12}\text{C}$
	$^{15}\text{O}$	2min2s	$(\gamma, n)$ on $^{16}\text{O}$
	$^{13}\text{N}$	10min	$(\gamma, n)$ on $^{14}\text{N}$
845.8	$^{27}\text{Mg}$	9min27s	n-capture on $^{26}\text{Mg}/(\text{n,p})$ on $^{27}\text{Al}$
	$^{57}\text{Mn}$	2h35min	$(\gamma, \text{p})$ on $^{57}\text{Fe}$ , $(\gamma, \text{n+p})$ on $^{58}\text{Fe}$ or n-capture on $^{55}\text{Mn}$
1271	$^{29}\text{Al}$	6min40s	$(\gamma, \text{p})$ on $^{30}\text{Si}$ or $(\text{n,p})$ on $^{29}\text{Si}$
1367	$^{24}\text{Na}$	15h	n-capture on $^{23}\text{Na}/(\gamma, \text{p})$ on $^{25}\text{Mg}$
1434	$^{52\text{m}}\text{Mn}$	21min7s	$(\text{p,n})$ on $^{52}\text{Cr}$
1460	$^{40}\text{K}$	1,27 billion y	n-capture on $^{39}\text{K}$
1776	$^{29}\text{Al}$	6min40s	$(\gamma, \text{p})$ on $^{30}\text{Si}$ or $(\text{n,p})$ on $^{29}\text{Si}$
1809	$^{56}\text{Mn}$	2h35min	$(\gamma, \text{p})$ on $^{56}\text{Fe}$ or n-capture on $^{55}\text{Mn}$
2164	$^{38}\text{K}$	7min56s	$(\gamma, n)$ on $^{39}\text{K}$
2422	$^{29}\text{Al}$	6min40s	$(\gamma, \text{p})$ on $^{30}\text{Si}$ or $(\text{n,p})$ on $^{29}\text{Si}$
2754	$^{24}\text{Na}$	15h	n-capture on $^{23}\text{Na} / (\gamma, \text{p})$ on $^{25}\text{Mg}$

#### 4. Conclusion

We irradiated a kimberlite sample using a 100 MeV electron beam to produce a bremsstrahlung radiation. Note that this energy is higher than the Mineral-PET energy, however this experiment gave a good idea of the different radioisotopes that would be produced during the activation process of Mineral-PET. We were able to unambiguously identify the contributors to the dominant gamma lines together with their lifetimes. A conclusive identification of some of the peaks could not be made because they were absorbed by noise. This is also the reason the lifetime spectra are taken after 10 min. The time taken to get the sample to the detectors and the initial period where the detectors are swamped were also taken into consideration. The use of the lifetime data can be seen here as a revolution in gamma-ray spectroscopy because without these data, many identifications would not have been possible. The next step in this analysis will be to identify all the remaining gamma lines, and based on the chemical composition of kimberlite use software like say FISPACT to inventory all the nuclear reactions that lead to the production of these radioisotopes.

#### References

- [1] M. S. H.O.A. Meyer, Natural Diamond, Ch. 10 in Handbook of industrial diamonds and diamond films (CRC Press, 1988).
- [2] G. Muehlelehner and J. Karp, Phys. Med. Biol. 51, R117 (2006).
- [3] G. C. Baldwin and G. S. Klaiber, Physical Review 711, 3 (1947).
- [4] Medhat et al, PRAMANA– Journal of Physics, Vol. 65, No 2 August 2005, pp.245-258
- [5] S. Ballestrero et al, CERN-Proceedings-2010-001: Proceedings of the 12th Varrenna Conference on Nuclear Reaction Mechanisms, July 2009.
- [6] [nucldata.nuclear.lu.se/toi/radSearch.asp](http://nucldata.nuclear.lu.se/toi/radSearch.asp) (last access on 17th July 2014)
- [7] T.R. Mcgetchin, The American Mineralogist, Vol 55, September-October 1970
- [8] Kenneth S. Krane, 1988. Introductory Nuclear physics. 1st ed. New York. John Wiley& Sons.